LAWRENCE
LIVERMORE
NATIONAL
LABORATORY

LLNL-JRNL-652320

Biomineralization of uranium by PhoY phosphatase activity aids cell survival in Caulobacter crescentus

M. C. Yung, Y. Jiao

March 26, 2014

Applied and Environmental Microbiology

Disclaimer

Biomineralization of uranium by PhoY phosphatase activity aids cell survival in *Caulobacter crescentus*.

Mimi C. Yung[1] and Yongqin Jiao[1,#]

[1]Biosciences and Biotechnology Division, Physical and Life Sciences Directorate, Lawrence Livermore National Laboratory, Livermore, California.

Running title: Uranium biomineralization by *Caulobacter*

Keywords: *Caulobacter crescentus*, uranium, uranium phosphate, aerobic uranium resistance, uranium biomineralization, phosphatase activity.

[#]Corresponding author. Address: Lawrence Livermore National Laboratory, 7000 East Avenue, L-452, Livermore, CA 94550; Phone: (925) 422-4482; Fax: (925) 422-2282; E-mail: jiao1@llnl.gov

ABSTRACT:

Caulobacter crescentus is known to tolerate high levels of uranium [U(VI)], but its detoxification mechanism is poorly understood. Here we show that *C. crescentus* is able to facilitate U(VI) biomineralization through the formation of U-P_i precipitates via its native alkaline phosphatase activity. The U-P_i precipitates, deposited on the cell surface in the form of meta-autunite structures, have a lower U/P_i ratio compared to chemically produced precipitates. The enzyme that is responsible for the phosphatase activity and thus the biomineralization process is identified as PhoY, a periplasmic, alkaline phosphatase with broad substrate specificity. Furthermore, PhoY is shown to confer a survival advantage to *C. crescentus* towards U(VI) under both growth and non-growth conditions. Results in this study thus highlight U(VI) biomineralization as a resistance mechanism in microbes, which not only improves our understanding of bacterial-mineral interactions, but also aids in defining potential ecological niches for metal-resistant bacteria.

INTRODUCTION:

Uranium (U) is a widespread environmental contaminant with major sources coming from energy and nuclear weapon production (1). With its oxidizing nature and high water solubility, hexavalent U(VI) is extremely toxic and carcinogenic (2). Chemical and physical techniques for waste treatment or removal of U are challenging and expensive. An alternative method for U remediation is microbially-mediated, *in situ* U immobilization, which has added benefits of reduced cost and environmental-friendliness relative to other approaches (3, 4).

The most studied form of microbial U(VI) immobilization is through microbial reduction by dissimilatory metal-reducing bacteria (DMRB) (5, 6). These organisms can directly or indirectly (*e.g.*, by coupling with iron or nitrate redox chemistry) reduce soluble U(VI) to less-soluble U(IV) under anaerobic conditions, resulting in immobilization. The biogenic U(IV) minerals (in the form of uraninite) generated by phylogenetically and metabolically diverse bacteria are chemically and structurally similar, suggesting a common mechanism for U(VI) reduction (7). Recent studies suggest that DMRB rely on high-molecular-weight, *c*-type cytochromes associated with the outer membrane for U(VI) reduction, similar to the reduction of other metals such as chromate and ferric iron (8). Many researchers have confirmed that uraninite is present both associated with the cell wall and in the periplasm (5, 9), with the exception of some rare reports of cytoplasmic uraninite, suggesting that U complexes do not generally have access to intracellular enzymes (10-12). The stability of thus-formed uraninite was later evaluated under environmental conditions. When exposed to oxygen or other electron acceptors, they are readily re-oxidized to the more mobile U(VI) form (13, 14), defeating the purpose of immobilization. Therefore, reduction of U(VI) is unlikely to be a successful long-term strategy for the immobilization of U.

Besides reductive precipitation under anaerobic conditions, other mechanisms of microbe-mediated U immobilization that are redox insensitive include reactions with enzymes or polysaccharides excreted on the cell surface by many microorganisms found in natural waters (15, 16). In particular, phosphatase activity, both acid and alkaline, from various bacterial species such as *Serratia* sp. N14 (formerly *Citrobacter* sp. N14), *Sphingomonas sp*. BSAR-1, *Arthrobacter* sp., *Rahnella* sp., and *Bacillus* sp. has been found to facilitate U(VI) precipitation through the formation of uranium phosphate complexes (17-19). Phosphatases from these organisms have been cloned and expressed in *Escherichia coli* and other organisms and the resulting engineered strains have been reported to efficiently precipitate uranium (20-22). Among all these systems, however, little attention was paid to the cellular benefits of the native or heterologously expressed phosphatases towards U(VI) resistance.

In this study, we examined the phosphatase-facilitated uranium tolerance mechanism in *Caulobacter crescentus* NA1000, providing a link between phosphatase activity, U biomineralization, and cell survival. *C. crescentus* is a ubiquitous, aerobic bacterium that is able to survive under low-nutrient conditions (23). *Caulobacter* species are able to tolerate high concentrations of U(VI) (24) and have been found in U contaminated sites (25). Exposure of *C. crescentus* to U(VI) has been shown to elicit U-specific cellular responses on both the transcriptional and proteomic levels (24, 26, 27). We show here for the first time that a ubiquitous organism like *C. crescentus* is able to tolerate uranium through its native phosphatase activity enabled by a periplasmic enzyme PhoY, demonstrating the potential for *C. crescentus* to be used for U(VI) bioremediation under aerobic conditions.

MATERIALS AND METHODS:

Materials, bacterial strains, and growth conditions.

All chemicals were purchased from Sigma-Aldrich (St. Louis, MO) unless otherwise noted. Peptone, yeast extract, and agar were purchased from Amresco (Solon, OH). Uranyl nitrate hexahydrate [$(UO_2)(NO_3)_2 \bullet 6H_2O$] was obtained from SPI Supplies (West Chester, PA). A stock solution of uranyl nitrate (100 mM) was prepared in 0.1 N nitric acid. All PCR reactions were amplified using iProof polymerase from Bio-Rad (Hercules, CA) supplemented with 5% dimethyl sulfoxide (DMSO) according to manufacturer's instructions. *Caulobacter crescentus* NA1000 was maintained on PYE-agar (0.2% peptone, 0.1% yeast extract with 0.5 mM $MgSO_4$, 1 mM $CaCl_2$, and 1.5% agar) (28). Liquid cultures were grown in either 1) PYE or 2) modified M5G minimal medium lacking inorganic phosphate (P_i) and containing 5 mM glycerol-2-phosphate as the sole phosphate source (M5G-GP, pH 7.0) (29). Where applicable, kanamycin was supplemented at 25 µg/mL in solid medium and 5 µg/mL in liquid medium for *C. crescentus* and 50 µg/mL in solid and liquid medium for *E. coli*.

For growth in PYE medium, *C. crescentus* cells were first pre-cultured in 2 mL of PYE from a single colony at 30 ^oC overnight. Saturated cultures were diluted to an initial optical density of 600 nm (OD_{600}) of 0.1 and cultured for an additional 2 h at 30 ^oC to an OD_{600} of 0.2, at which point uranyl nitrate was added to the medium to a final concentration of 200 µM. Cells were grown for an additional 30 min after which culture was analyzed. Growth of cells was performed in biological triplicate and monitored using OD_{600}.

For growth in M5G-GP medium, *C. crescentus* cells were pre-cultured in 2 mL of PYE or PYE supplemented with kanamycin when appropriate from single colonies at 30 ^oC overnight. Saturated cultures were diluted in the morning in PYE to an initial OD_{600} of 0.04 and incubated

98 for another 7 h until OD_{600} was about 0.5 (late exponential phase). Cells were harvested, washed
99 once with 10 mM NaCl, and inoculated into M5G-GP supplemented with 0 or 50 μM uranyl
100 nitrate to an initial OD_{600} of 0.02. M5G-GP media were not supplemented with kanamycin due
101 to kanamycin inactivation by uranium (data not shown). Growth of cells was performed in
102 biological triplicate and monitored using OD_{600}.
103
104 ***Construction of ΔphoY.***
105 The ~400 bp regions upstream and downstream of the *phoY* open reading frame
106 (CCNA_02545) were PCR amplified and cloned into pNPTS138 (M. K. Alley, unpublished).
107 The upstream fragment was amplified using primers phoY_URfor and phoY_URrev (Integrated
108 DNA Technologies, Coralville, IA), and the downstream fragment was amplified using primers
109 phoY_DRfor and phoY_DRrev (Table 2). A three-way Gibson assembly (Clontech In-Fusion
110 HD Cloning Plus kit, Mountain View, CA) of the upstream and downstream fragments into the
111 HindIII and EcoRI sites of pNPTS138 generated pMCY10 (Table 1). Confirmation of the
112 plasmid was determined by DNA sequencing. An in-frame deletion of *phoY* (YJ0010, Table 1)
113 was generated using pMCY10 through standard homologous recombination methods as
114 previously described (30, 31). Deletion of *phoY* was confirmed by DNA sequencing (Elim
115 Biopharmaceuticals, Hayward, CA).
116
117 ***Construction of phoY complement and phoY-mcherry strains.***
118 To generate the *phoY* complement strain, the *phoY* open reading frame was first PCR
119 amplified using primers BXphoY_for and BXphoY_rev (Table 2). The *phoY* fragment was then
120 inserted in frame using Gibson assembly into the NdeI and EcoRI sites downstream of the

121 xylose-inducible promoter (P_{xyl}) in pBXMCS-2 (32) to generate pMCY21 (Table 1), which was
122 confirmed by DNA sequencing. Δ*phoY* mutant was transformed with pMCY21 to obtain the P_{xyl}
123 *phoY* complement strain YJ0021. Transformants were selected on PYE-agar supplemented with
124 kanamycin.

125 To generate the *phoY-mcherry* strain, the *phoY* open reading frame was PCR amplified
126 using primers RVphoY_for and RVphoY (Table 2). This *phoY* fragment was inserted using
127 Gibson assembly into the NdeI and EcoRI sites upstream of the *mcherry* coding region in
128 pRVCHYC-2 (32). The resulting *phoY-mcherry* construct was then PCR amplified using
129 primers BXphoY_for and BXphoYch_rev (Table 2) and was subsequently inserted into the NdeI
130 and XbaI sites downstream of the P_{xyl} promoter in pBXMCS-2 (32) to generate pMCY23 (Table
131 1). Confirmation of the plasmid was determined by DNA sequencing. Δ*phoY* was transformed
132 with pMCY23 to obtain the P_{xyl} *phoY-mcherry* strain YJ0023. Transformants were selected on
133 PYE-agar supplemented with kanamycin. Experiments with YJ0021 and YJ0023 were
134 conducted without xylose supplementation since leaky expression from the xylose promoter
135 provided sufficient PhoY activity.

136

137 ***Cell-bound phosphatase assay.***

138 *C. crescentus* NA1000 was grown in PYE with and without U addition as described
139 above. Cells were harvested, washed once with 10 mM NaCl, and re-suspended in 100 mM
140 Tris-HCl pH 7.0 to a final OD_{600} of 0.5 in a final volume of 700 µL. Phosphatase assays were
141 started by addition of glucose-6-phosphate, fructose-1,6-bisphosphate, or glycerol-2-phosphate
142 to a final concentration of 5 mM. At each time point, aliquots of assays were removed to
143 quantitate the total P_i content as described below.

144

145 ***U biomineralization assay.***

146 *C. crescentus* NA1000, YJ0010 (Δ*phoY*), and YJ0021 (Δ*phoY*/pMCY21) cells were
147 individually pre-cultured in 500 μL of PYE or PYE supplemented with kanamycin from single
148 colonies at 30 ^{o}C for 8 h. Cells were then diluted to an initial OD_{600} of 0.001 and cultured for 16
149 h until the OD_{600} was about 0.6 (late exponential phase). Cells were harvested, washed once
150 with 10 mM NaCl, and re-suspended in 50 mM PIPES pH 7.0 to a final OD_{600} of 0.5 in a final
151 volume of 700 μL. Biomineralization assays were started by the addition of glycerol-2-
152 phosphate and uranyl nitrate to final concentrations of 5 mM and 500 μM, respectively, and
153 incubated at 30 ^{o}C. We note that U(VI) is fully soluble under these assay conditions, presumably
154 by complexation with glycerol-2-phosphate. Controls without glycerol-2-phosphate or uranyl
155 nitrate were also conducted. At each assay time point, aliquots were removed to quantitate the
156 total, soluble, and insoluble U and P_i content as described below. Aliquots were also removed
157 for cell survival analysis. Serial dilutions of 10^1 to 10^6 of the aliquots were prepared in PYE and
158 10 μL of each dilution were spotted on PYE-agar. Images of the spots were taken after 2 days of
159 incubation at 30 ^{o}C.

160

161 ***Measurement of U and P_i.***

162 To measure total U and P_i content, 45 μL of sample was directly quenched with 45 μL of
163 12.5% trichloroacetic acid (TCA). Samples were centrifuged at 20,000 x *g* to remove cell debris
164 and supernatant was analyzed for total U and P_i via Arsenazo III and molybdate colorimetric
165 assays, respectively (33, 34). Briefly, to measure U, 40 μL of supernatant was added to 60 μL of
166 filtered 0.1% Arsenazo III in 6.25% TCA. Absorbance at 652 nm was measured and compared

to standards to determine the U concentration. To measure P_i, 40 μL of supernatant was added to 60 μL of 1% ammonium molybdate and 7.2% $FeSO_4$ in 3.2% H_2SO_4. Absorbance at 700 nm was measured and compared to standards to determine the P_i concentration.

To measure soluble U and P_i content, 45 μL of sample was immediately centrifuged at 20,000 x *g* for 5 min. Supernatant was quenched with an equal volume of 12.5% TCA and then analyzed for soluble U and P_i concentrations as described above. To measure the insoluble U and Pi content, the pellet after centrifugation was re-suspended in 45 μL of degassed 300 mM $NaHCO_3$ in water and mixed at room temperature for 5 min. Sample was then centrifuged again at 20,000 x *g* for 5 min. Supernatant was quenched with an equal volume of 12.5% TCA and analyzed for U and P_i concentrations as described above.

XRD sample preparation and analysis.

For XRD analysis, 40 mL of cell culture grown with 200 μM U in PYE for 30 min was harvested by centrifugation at 20,000 x *g* for 10 min. The pellet was washed with water three times. Clear separation of cells and precipitates was observed. The top layer of cells was re-suspended in residual liquid by gentle pipetting and carefully removed. The bottom layer was re-suspended in water, spread on an XRD disk, and dried overnight in a desiccated chamber. To control for chemical and cell-surface induced precipitation, abiotic and heat-killed cell controls were included. The heat-killed cell sample was prepared by heating cells at 70 ^{o}C for 10 min. XRD analysis was performed on a Bruker D8 X-ray defractometer (Billerica, MA), and spectra were compared to references from the International Centre for Diffraction Data (ICDD).

TEM sample preparation and imaging.

For cells grown with 200 μM U in PYE medium for 30 min, 3 mL of culture was used. For cells originating from U biomineralization assays, 1.6 mL of cell suspension at 5 h assay time with 5 mM glycerol-2-phosphate and 250 μM uranyl nitrate was collected.

Samples were harvested at 20,000 x *g* for 1 min and fixed in 1 mL of 4% (w/v) paraformaldehyde in 100 mM sodium cacodylate pH 7.2 for 1 h at room temperature with rocking. The pellet was washed once with 1 mL of water and then dehydrated sequentially in 1 mL of each of the following for 10 min: 50% ethanol, 70% ethanol, 90% ethanol, and 100% ethanol. The 100% ethanol dehydration was repeated twice. The cell pellet was then dislodged in 1 mL of 50% LR White resin (Electron Microscopy Sciences, Hatfield, PA) in ethanol and incubated at room temperature overnight with rocking, protected from light. Cell pellet was then infiltrated with 1 mL of fresh 100% LR White for 1 h at room temperature two times. Finally, cells were embedded in LR White anaerobically at 65 ^{o}C for 2 days.

Thin sections of 90 nm thickness were cut from embedded samples using a Leica Ultracut UC6 ultramicrotome (Buffalo Grove, IL) with a diamond knife. Sections were collected using 200 mesh, Formvar/carbon-coated, copper grids (Ted Pella, Redding, CA). Transmission electron microscopy (TEM) was conducted using a FEI/Philips CM300 transmission electron microscope equipped with energy-dispersive X-ray spectroscopy (EDS). Images were collected at an accelerating voltage of 300 kV.

Fluorescence microscopy.

Strain YJ0023 (Δ*phoY*/pMCY23) was cultured from a single colony at 30 ^{o}C in PYE supplemented with kanamycin until the cells reached an OD_{600} of 0.25 (mid exponential phase).

213 Cells were harvested and re-suspended in 1/10 of the culture volume. Five microliters of the
214 concentrated cells were spotted on a PYE-1% agarose pad and imaged using an Axiovert 200M
215 microscope (Zeiss, Minneapolis, MN) equipped with a Photometric CoolSNAP HQ CCD
216 camera. Images were acquired with a 100x objective and a Texas Red filter set (Chroma,
217 Bellows Falls, VT, filter #41004). Images were processed using ImageJ (35).
218
219 **RESULTS:**
220 ***Caulobacter produces extracellular, crystalline U-P_i precipitates.***
221 To determine if *C. crescentus* is able to facilitate uranium phosphate (U-P_i) precipitation,
222 wild type strain NA1000 was grown in PYE medium to early-exponential phase at which time
223 uranyl nitrate was added to a final concentration of 200 μM. After an additional 30 min, the
224 concentrations of uranium and phosphate present in the soluble and insoluble fractions were
225 determined (Table 3). As a control for chemical precipitation, abiotic samples with no cells were
226 also prepared.
227 The biotic, cell-containing samples showed higher amounts of both uranium and
228 phosphate in the insoluble fraction (154 ± 2 μM U and 172 ± 8 μM P_i) compared to that of the
229 abiotic control (108 ± 11 μM U and 83 ± 16 μM P_i), suggesting that cell metabolism induces U-
230 P_i precipitation (Table 3). The higher amount of U present in the biotic insoluble fraction is
231 consistent with the lower U concentration in the soluble fraction. The concentration of P_i in all
232 fractions (soluble, insoluble and total) are higher for the biotic versus abiotic samples, indicating
233 that P_i was produced and released from cells during growth. P_i production by *C. crescentus*
234 during growth was confirmed by monitoring P_i concentration in the medium throughout growth
235 in the absence of U (data not shown). The fact that the insoluble P_i makes up a greater
236 proportion of the total P_i in the biotic sample compared to the abiotic sample (22 ± 2% versus 13

± 3%) indicates that some of the P_i produced by the cells is precipitated in the insoluble fraction. Further calculations indicate that the biotic sample had a lower molar ratio of U to P_i in the insoluble fraction compared to that of the abiotic sample (Table 3), suggesting that the biotic precipitates may be chemically different from the abiotic precipitates and that the cellular production of P_i is responsible for the biomineralization process.

XRD analysis was used to determine the crystallinity and identity of the U precipitates. Only precipitates produced in the presence of cells generated a diffraction pattern, indicative of crystalline material (Fig. 1A); samples from abiotic or heat killed cells did not produce any detectable diffraction pattern. The XRD spectrum of the biotic precipitates confirmed the presence of meta-autunite (uranyl phosphate species in the U(VI) oxidation state), present likely in the form of uramphite ($(NH_4)(UO_2)(PO_4)\bullet 3H_2O$, ICDD 00-042-0384), potassium sodium uranyl phosphate hydrate ($(Na_{0.43}K_{0.57}(UO_2)(PO_4)\bullet 3+xH_2O$, ICCD 00-059-0399), and/or potassium uranyl phosphate hydrate ($K(UO_2)(PO_4)\bullet 3H_2O$, ICCD 00-049-0433).

In order to determine where uranium precipitates reside relative to cells, TEM analysis of the samples collected after 30 min U exposure was performed. The majority of the precipitates were found to be located extracellularly in the bulk medium (Fig. 1B). Occasionally, we observed precipitates surrounding the surface of the cells (Fig. 1C). EDS analysis revealed that all precipitates contained primarily U and P (Fig. 1D). Based on peak intensity of the EDS spectrum, the cell surface-associated precipitates appear to have a lower U to P ratio compared to those present in the bulk medium. While the lower U/P ratio may be indicative of the P_i released and precipitated with U on the cell surface, the presence of phosphate-containing macromolecules on the cell surface such as lipopolysaccharides and phospholipids may also

contribute to the lower ratio. The interior of the cells appears to have negligible amounts of U, but significant amounts of P as expected given the prevalence of P in proteins and nucleotides.

Uranium biomineralization is catalyzed by PhoY.

Given that uranium precipitates formed in presence of cells contain higher amounts of P_i compared to the abiotic control (Table 3), we hypothesized that P_i production by phosphatases facilitates U biomineralization, which has been observed in other systems (17-19). Whole-cell phosphatase activity of *C. crescentus* grown in PYE with and without U was tested with three different organic phosphate substrates: glucose-6-phosphate, fructose-1,6-bisphosphate, and glycerol-2-phosphate (Fig. S1). The results revealed phosphatase activity towards all three substrates, indicating broad substrate specificity. Surprisingly, cells grown with and without U exhibited the same phosphatase activity towards each substrate tested (Fig. S1), indicating that phosphatase activity is neither induced nor inhibited by U. In addition, we found no evidence for extracellular phosphatase activity in the spent medium with and without U (data not shown), confirming that the phosphatase activity is cell-bound.

To identify the gene(s) encoding the enzyme(s) responsible for the whole-cell phosphatase activity and thus the U biomineralization observed, we searched the annotated genome of *C. crescentus* for alkaline phosphatases (36). We focused on alkaline instead of acid phosphatases because the activities that we observed had an optimal pH of 7.5 (Fig. S2). A genome search revealed 4 annotated alkaline phosphatases in *C. crescentus* NA1000. Based on TEM and activity assay results, we hypothesized that the cellular location of the responsible phosphatase would be non-cytoplasmic. Therefore, each of the 4 annotated proteins was analyzed for an N-terminal export signal sequence using SignalP 4.1 (37). Only CCNA_02545

(herein named PhoY) had a predicted signal sequence for export across the cytoplasmic membrane. In addition, the prokaryote subcellular protein localization tool PSORT (38) predicted with 98% expected accuracy that PhoY is a periplasmic protein. To experimentally test the bioinformatics prediction, we constructed a xylose-inducible *phoY-mcherry* fusion strain. Fluorescence microscopy revealed that PhoY-mCherry was indeed localized to the cell periphery (Fig. 2). We should note that there is a slight discrepancy in the translational start site of PhoY in the currently available versions of genome annotation for *C. crescentus* in NCBI (36, 39). However, this discrepancy does not affect the mature protein sequence and thus the results of this study. Phylogenetic analysis of the mature protein sequence of PhoY (Fig. S3) revealed that it is most similar to PhoK in *Sphingomonas* sp. BSAR-1 (39% identity, 51% similarity), an alkaline phosphatase previously shown to catalyze U biomineralization (18). However, notably, the pH optimum for phosphatase activity in *C. crescentus* (pH 7.5) differs significantly from that of *Sphingomonas* sp. BSAR-1 (pH 9.0) (Fig. S2) (18). Nevertheless, PhoY and PhoK belong to a group that is clearly distinct from acid phosphatases (*e.g.,* PhoN in *Salmonella enterica*) that have been implicated in U biomineralization as well as other annotated phosphatases in *C. crescentus* (17, 19, 20).

In order to test if PhoY is responsible for U biomineralization in *C. crescentus*, we compared the abilities of wild type NA1000 and a PhoY deletion mutant (Δ*phoY*) to biomineralize U (Fig. 3). The biomineralization assay was conducted with glycerol-2-phosphate as the organic phosphate source at pH 7.0 in order to prevent chemical precipitation of U. Wild type cells clearly exhibited biomineralization activity as evidenced by the decrease in soluble U and increase of insoluble U over time (Fig. 3). Although both the soluble and total P_i concentrations increased over time, the soluble P_i was consistently lower than the total P_i,

consistent with the increase in insoluble P_i. In controls without glycerol-2-phosphate, no P_i production or U precipitation was observed as expected (Fig. S4). In contrast to wild type, Δ*phoY* did not produce any P_i nor precipitate any U, indicating PhoY is responsible for the whole-cell phosphatase activity and U biomineralization in *C. crescentus*. Furthermore, a complement strain (YJ0023) in which Δ*phoY* harbors a xylose inducible *phoY* plasmid rescued the P_i production and U precipitation. Notably, the complement strain has a higher phosphatase activity (480 ± 10 nmol/h) than wild type (260 ± 10 nmol/h). As a result, the rate of U precipitation was faster in the complement strain (136 ± 3 nmol/h) than in wild type (80 ± 10 nmol/h). Comparison of P_i production with and without U confirmed that the presence of U did not affect phosphatase activity (Fig. S5), demonstrating that endogenous phosphatase activity is responsible for U biomineralization.

To further examine the U biomineralization process, we performed TEM analyses of samples collected at the 5 h time point of the biomineralization assay (Fig. 3F). TEM images of both wild type and the *phoY* complement strains revealed the presence of extracellular U-P_i precipitates. In contrast, Δ*phoY* was bare of extracellular precipitates. Intracellular dark deposits appear to be present in Δ*phoY* and EDS analysis revealed that these deposits do contain U (data not shown). However, due to the weak contrast of the image and potential non-specific staining inherent to TEM sample preparation, we cannot exclude the possibility that these dark deposits are artifacts.

PhoY aids cell survival under U exposure.

Several studies have established that phosphatase activity facilities U biomineralization (17-19), however, few studies have directly examined whether the biomineralization process

affects cell survival and function (40). To address this question, we compared both growth and cell survival of wild type, Δ*phoY*, and the *phoY* complement strain under U biomineralization conditions. Growth tests in M5G-GP medium with glycerol-2-phosphate as the sole phosphate source indicated that while all three strains grew well in the absence of U, only Δ*phoY* showed lack of growth in the presence of U (Fig. 4). The initial growth lag observed with Δ*phoY* in the absence of U is likely caused by P_i limitation due to lack of extracellular phosphatase activity. The fact that the Δ*phoY* strain eventually grew suggests the presence of alternative phosphatases. We suspect *C. crescentus* is able to transport glycerol-2-phosphate into the cell and generate P_i through intracellular phosphatases as an alternative pathway to obtain P_i for growth. Consistently, we did not observe P_i accumulation in the medium with Δ*phoY* with or without U (data not shown). Notably, PhoY-stimulated growth under U only occurs when P_i is initially absent in the growth medium; we observed no difference in growth between wild type and Δ*phoY* in PYE medium with and without U (Fig. S6).

To test PhoY-induced cell survival during U exposure under non-growth conditions, aliquots of wild type, Δ*phoY*, and the *phoY* complement strain during the biomineralization assay were serially diluted and spotted on PYE-agar to test for survival (Fig. 3E). Controls with no glycerol-2-phosphate or U were included for comparison. Compared to wild type, Δ*phoY* exhibited a ~100 fold increase in cell death at 7.5 h, demonstrating that PhoY confers a survival advantage during U exposure under non-growth conditions. The *phoY* complement strain restored survival in the biomineralization assay; no significant cell death was observed compared to the no U control. We note that the *phoY* complement strain did exhibit a general survival disadvantage in the absence of U, which is likely attributed to metabolic burden and/or toxicity from PhoY overexpression, consistent with the strain's slower growth in M5G-GP medium (Fig.

351 4). Finally, the most severe cell death was observed for all strains in controls with U alone and
352 without glycerol-2-phosphate, with almost complete cell death after 1.5 h. This observation
353 suggests that free uranyl-nitrate species in solution is more toxic than U complexed with
354 glycerol-2-phosphate, which in turn is more toxic than U-P_i precipitates. These results thus
355 highlight the importance of speciation when examining U toxicity to microbes.
356
357 **DISCUSSION:**
358 In this study, we demonstrated that a ubiquitous organism, *Caulobacter crescentus*, is
359 able to catalyze the formation of uranium phosphate precipitates at the cell surface when exposed
360 to U(VI). The biogenic U precipitates are crystalline with a higher P/U ratio than chemically
361 produced precipitates, characteristics that may allow analytical differentiation of the biogenic
362 minerals from their abiotic counterparts found in the environment. XRD analysis showed that
363 the precipitates are in the form of meta-autunite, with no alteration of the U(VI) redox state
364 during the biomineralization process, in contrast to the reductive precipitation by DMRB under
365 anaerobic conditions (5, 13). Immobilization of U as U(VI) phosphate minerals under aerobic
366 conditions offers the possibility of long-term U stability since meta-autunite minerals have been
367 shown to be stable for long periods of time, over a wide range of pH (41). These results thus
368 highlight the potential utility of *C. crescentus* for U immobilization in the oxic zones of
369 contaminated sites.
370 Based on results described in this study, we propose a model for U biomineralization by
371 *C. crescentus* (Fig. 5), in which the non-specific, alkaline phosphatase PhoY is responsible for
372 the production of P_i in the periplasm, which in turn precipitates with U(VI) to form meta-autunite
373 minerals on the cell surface and in the bulk medium. While the cell surface deposited uranium

374 phosphate precipitates observed by TEM (Fig. 1) likely result from *in situ* precipitation
375 facilitated by PhoY, we cannot exclude other possibilities. U is known to interact with bacterial
376 cell surfaces through interaction with phosphate-containing macromolecules such as LPS and S-
377 layer (42, 43). S-layer protein has been shown to be important for U resistance in *Bacillus*
378 *sphaericus* JG-7B (43); however, it does not appear to contribute significantly to U
379 immobilization or cell survival in *C. crescentus* (Fig. S7). This difference is probably due to
380 lack of phosphorylated S-layer protein in *C. crescentus*, in contrast to *B. sphaericus* (43).

381 Remarkably, PhoY-induced U biomineralization aids survival of *C. crescentus* toward U
382 under both growth and non-growth conditions. Given the periplasmic localization of PhoY, we
383 hypothesize that the production of P_i by PhoY impedes U transport into the cytoplasm by local
384 precipitation in the periplasm as a first line of defense, preventing U toxicity to the organism.
385 TEM images showing a lack of intracellular uranium deposits in wild type and the *phoY*
386 complement strain support this hypothesis (Fig. 3). It is becoming apparent that biominerals
387 produced by certain organisms, ranging from prokaryotes to eukaryotes, play an important
388 protective role by acting as critical detoxification sinks to efficiently remove potentially toxic
389 species from the immediate environment (44, 45). Surprisingly, however, the phosphatase
390 activity in *C. crescentus* is not induced by the presence of U, suggesting that U biomineralization
391 is likely a fortuitous consequence of native phosphatase activity.

392 Another example that reflects the intricacy between U resistance and phosphate
393 metabolism in *C. crescentus* is the role of a phytase enzyme (CCNA_01353), previously found to
394 be up-regulated in response to U and able to facilitate growth in U when phytate served as the
395 sole phosphate source (24, 27). The protection mechanism by the phytase, however, is likely
396 different from that of the PhoY phosphatase presented in this study. In the case of phytase, we

found no detectable amount of P_i released into the medium and no U precipitation from wild type cells grown in the presence of U with phytate as the sole phosphate source (data not shown). Furthermore, phytase activity was found to be 10 times lower than the PhoY activity in whole-cell assays (data not shown), which may explain why almost no U biomineralization was detected. Thus the protective role of phytase is likely through supply of P_i for growth under these conditions rather than U biomineralization.

In the PhoY system, in contrast, cells do not experience significant P_i limitation, due to the presence of highly-active PhoY and/or other intracellular phosphatases, as evidenced by the normal growth rate of Δ*phoY* in glycerol-2-phosphate in the absence of U. Thus, supply of P_i for growth is unlikely the primary mechanism for resistance. We hypothesize that U biomineralization by PhoY is likely the primary mechanism for resistance through a precipitation-induced shift of U speciation. Consistently, the increase in cell survival by the presence of PhoY was not apparent until sufficient P_i was produced and U was biomineralized (Fig. 3). Although the relationship between U speciation and bioavailability is complex (1), there is reasonable evidence to indicate that free UO_2^{2+} and UO_2OH^+ are the major forms of U(VI) available to organisms, rather than U in chelation complexes or adsorbed to colloidal and/or particulate matter (4). Consistently, our results showed that U(VI) complexes with both organic and inorganic forms of phosphate greatly reduce U toxicity, with the inorganic phosphate form being the least toxic (Fig. 3). By converting organic phosphates to inorganic phosphates, PhoY shifts the pool of U from chelating with organic phosphate to precipitation with inorganic phosphate, resulting in a decrease in U toxicity.

The findings presented in this study help define and characterize biogenic U minerals as well as U trafficking during biomineralization in *C. crescentus*, establishing a model for this

process (Fig. 5) and demonstrating the potential utility of this organism in U bioremediation. We further identified PhoY as an alkaline phosphatase that plays a central role in U biomineralization and resistance. Knowledge gained in this study thus not only improves our understanding of bacteria-mineral interactions on the surfaces of metal-resistant bacteria, but also helps us in defining ecological niches for metal-resistant bacteria.

ACKNOWLEDGEMENTS:

We thank Mavrik Zavarin for assistance with XRD analysis. We thank Mark Wall for help with TEM-EDS analysis. We thank Catherine Lacayo for help with fluorescence microscopy. We thank Dan Park for critical review of the manuscript. This work was performed under the auspices of the U.S. Department of Energy by Lawrence Livermore National Laboratory under Contract DE-AC52-07NA27344 (LLNL-JRNL-652320). This study was supported by a Department of Energy Early Career Research Program award from the Office of Biological and Environmental Sciences (to Y.J.).

REFERENCES:

1. **Markich SJ.** 2002. Uranium speciation and bioavailability in aquatic systems: an overview. TheScientificWorldJournal **2:**707-729.

2. **NRC.** 2008. Review of toxicologic and radiologic risks to military personnel from exposure to depleted uranium during and after combat. The National Academies Press, Washington, DC.

441 3. **Phillips EJP, Landa ER, Lovley DR.** 1995. Remediation of uranium contaminated soils
442 with bicarbonate extraction and microbial U(VI) reduction. J. Ind. Microbiol. **14:**203-
443 207.
444 4. **Turick CE, Knox AS, Leverette CL, Kritzas YG.** 2008. In situ uranium stabilization
445 by microbial metabolites. J Environ Radioactiv **99:**890-899.
446 5. **Wall JD, Krumholz LR.** 2006. Uranium reduction. Annu. Rev. Microbiol. **60:**149-166.
447 6. **Williams KH, Bargar JR, Lloyd JR, Lovley DR.** 2013. Bioremediation of uranium-
448 contaminated groundwater: a systems approach to subsurface biogeochemistry. Curr.
449 Opin. Biotechnol. **24:**489-497.
450 7. **Sharp JO, Schofield EJ, Veeramani H, Suvorova EI, Kennedy DW, Marshall MJ,**
451 **Mehta A, Bargar JR, Bernier-Latmani R.** 2009. Structural similarities between
452 biogenic uraninites produced by phylogenetically and metabolically diverse bacteria.
453 Environ. Sci. Technol. **43:**8295-8301.
454 8. **Marshall MJ, Beliaev AS, Dohnalkova AC, Kennedy DW, Shi L, Wang Z, Boyanov**
455 **MI, Lai B, Kemner KM, McLean JS, Reed SB, Culley DE, Bailey VL, Simonson CJ,**
456 **Saffarini DA, Romine MF, Zachara JM, Fredrickson JK.** 2006. c-Type cytochrome-
457 dependent formation of U(IV) nanoparticles by *Shewanella oneidensis*. PLoS Biol.
458 **4:**e268.
459 9. **Xu H, Barton L, Zhang P, Wang Y.** 2000. TEM investigation of U^{6+} and Re^{7+} reduction
460 by *Desulfovibrio desulfuricans*, a sulfate-reducing bacterium. Mat. Res. Soc. Symp. Proc.
461 **608:**299-304.
462 10. **Suzuki Y, Kelly SD, Kemner KM, Banfield JF.** 2004. Enzymatic U(VI) reduction by
463 *Desulfosporosinus* species. Radiochim. Acta **92:**11-16.

11. **Liu C, Gorby YA, Zachara JM, Fredrickson JK, Brown CF.** 2002. Reduction kinetics of Fe(III), Co(III), U(VI), Cr(VI), and Tc(VII) in cultures of dissimilatory metal-reducing bacteria. Biotechnol. Bioeng. **80:**637-649.

12. **Lovley DR, Phillips EJ.** 1992. Reduction of uranium by *Desulfovibrio desulfuricans*. Appl. Environ. Microbiol. **58:**850-856.

13. **Senko JM, Istok JD, Suflita JM, Krumholz LR.** 2002. In-situ evidence for uranium immobilization and remobilization. Environ. Sci. Technol. **36:**1491-1496.

14. **Finch R, Murakami T.** 1999. Systematics and paragenesis of uranium minerals, p. 221-253. *In* Burns PC, Finch R (ed.), Uranium: minerology, geochemistry and the environment, vol. 38. Minerological Society of America, Washington, DC.

15. **Kalin M, Wheeler WN, Meinrath G.** 2005. The removal of uranium from mining waste water using algal/microbial biomass. J Environ Radioactiv **78:**151-177.

16. **Haferburg G, Kothe E.** 2007. Microbes and metals: interactions in the environment. J. Basic Microbiol. **47:**453-467.

17. **Macaskie LE, Bonthrone KM, Rouch DA.** 1994. Phosphatase-mediated heavy metal accumulation by a *Citrobacter* sp. and related enterobacteria. FEMS Microbiol. Lett. **121:**141-146.

18. **Nilgiriwala KS, Alahari A, Rao AS, Apte SK.** 2008. Cloning and overexpression of alkaline phosphatase PhoK from *Sphingomonas* sp. strain BSAR-1 for bioprecipitation of uranium from alkaline solutions. Appl. Environ. Microbiol. **74:**5516-5523.

19. **Martinez RJ, Beazley MJ, Taillefert M, Arakaki AK, Skolnick J, Sobecky PA.** 2007. Aerobic uranium (VI) bioprecipitation by metal-resistant bacteria isolated from radionuclide- and metal-contaminated subsurface soils. Environ. Microbiol. **9:**3122-3133.

20. **Basnakova G, Stephens ER, Thaller MC, Rossolini GM, Macaskie LE.** 1998. The use of *Escherichia coli* bearing a *phoN* gene for the removal of uranium and nickel from aqueous flows. Appl. Microbiol. Biotechnol. **50:**266-272.

21. **Powers LG, Mills HJ, Palumbo AV, Zhang C, Delaney K, Sobecky PA.** 2002. Introduction of a plasmid-encoded *phoA* gene for constitutive overproduction of alkaline phosphatase in three subsurface *Pseudomonas* isolates. FEMS Microbiol. Ecol. **41:**115-123.

22. **Kulkarni S, Ballal A, Apte SK.** 2013. Bioprecipitation of uranium from alkaline waste solutions using recombinant *Deinococcus radiodurans*. J. Hazard. Mater. **262:**853-861.

23. **Laub MT, Shapiro L, McAdams HH.** 2007. Systems biology of *Caulobacter*. Annu. Rev. Genet. **41:**429-441.

24. **Hu P, Brodie EL, Suzuki Y, McAdams HH, Andersen GL.** 2005. Whole-genome transcriptional analysis of heavy metal stresses in *Caulobacter crescentus*. J. Bacteriol. **187:**8437-8449.

25. **Utturkar SM, Bollmann A, Brzoska RM, Klingeman DM, Epstein SE, Palumbo AV, Brown SD.** 2013. Draft genome sequence for *Caulobacter* sp. strain OR37, a bacterium tolerant to heavy metals. Genome Announc. **1:**e00322-00313.

26. **Hillson NJ, Hu P, Andersen GL, Shapiro L.** 2007. *Caulobacter crescentus* as a whole-cell uranium biosensor. Appl. Environ. Microbiol. **73:**7615-7621.

27. **Yung MC, Ma J, Salemi MR, Phinney BS, Bowman GR, Jiao Y.** 2014. Shotgun proteomic analysis unveils survival and detoxification strategies by *Caulobacter crescentus* during exposure to uranium, chromium, and cadmium. J. Proteome Res. **ASAP:**DOI: 10.1021/pr400880s.

28. **Ely B.** 1991. Genetics of *Caulobacter crescentus*. Meth. Enzymol. **204:**372-384.

29. **Domian IJ, Quon KC, Shapiro L.** 1997. Cell type-specific phosphorylation and proteolysis of a transcriptional regulator controls the G1-to-S transition in a bacterial cell cycle. Cell **90:**415-424.

30. **Ried JL, Collmer A.** 1987. An *nptI-sacB-sacR* cartridge for constructing directed, unmarked mutations in gram-negative bacteria by marker exchange-eviction mutagenesis. Gene **57:**239-246.

31. **Stephens C, Reisenauer A, Wright R, Shapiro L.** 1996. A cell cycle-regulated bacterial DNA methyltransferase is essential for viability. Proc. Natl. Acad. Sci., USA **93:**1210-1214.

32. **Thanbichler M, Iniesta AA, Shapiro L.** 2007. A comprehensive set of plasmids for vanillate- and xylose-inducible gene expression in *Caulobacter crescentus*. Nucleic Acids Res. **35:**e137.

33. **Holman WI.** 1943. A new technique for the determination of phosphorus by the molybdenum blue method. Biochem. J. **37:**256-259.

34. **Fritz JS, Bradford EC.** 1958. Detection of thorium and uranium. Anal. Chem. **30:**1021-1022.

35. **Schneider CA, Rasband WS, Eliceiri KW.** 2012. NIH image to ImageJ: 25 years of image analysis. Nature methods **9:**671-675.

36. **Nierman WC, Feldblyum TV, Laub MT, Paulsen IT, Nelson KE, Eisen JA, Heidelberg JF, Alley MR, Ohta N, Maddock JR, Potocka I, Nelson WC, Newton A, Stephens C, Phadke ND, Ely B, DeBoy RT, Dodson RJ, Durkin AS, Gwinn ML, Haft DH, Kolonay JF, Smit J, Craven MB, Khouri H, Shetty J, Berry K, Utterback**

T, Tran K, Wolf A, Vamathevan J, Ermolaeva M, White O, Salzberg SL, Venter JC, Shapiro L, Fraser CM. 2001. Complete genome sequence of *Caulobacter crescentus*. Proc. Natl. Acad. Sci. U. S. A. **98:**4136-4141.

37. **Petersen TN, Brunak S, von Heijne G, Nielsen H.** 2011. SignalP 4.0: discriminating signal peptides from transmembrane regions. Nat. Methods **8:**785-786.

38. **Yu NY, Wagner JR, Laird MR, Melli G, Rey S, Lo R, Dao P, Sahinalp SC, Ester M, Foster LJ, Brinkman FSL.** 2010. PSORTb 3.0: improved protein subcellular localization prediction with refined localization subcategories and predictive capabilities for all prokaryotes. Bioinformatics **26:**1608-1615.

39. **Ely B, Scott LE.** 2014. Correction of the *Caulobacter crescentus* NA1000 genome annotation. PloS one **9:**e91668.

40. **Plummer EJ, Macaskie LE.** 1990. Actinide and lanthanum toxicity towards a Citrobacter sp.: uptake of lanthanum and a strategy for the biological treatment of liquid wastes containing plutonium. Bull. Environ. Contam. Toxicol. **44:**173-180.

41. **Beazley MJ, Martinez RJ, Webb SM, Sobecky PA, Taillefert M.** 2011. The effect of pH and natural microbial phosphatase activity on the speciation of uranium in subsurface soils. Geochim. Cosmochim. Acta **75:**5648-5663.

42. **Barkleit A, Foerstendorf H, Li B, Rossberg A, Moll H, Bernhard G.** 2011. Coordination of uranium(VI) with functional groups of bacterial lipopolysaccharide studied by EXAFS and FT-IR spectroscopy. Dalton Trans. **40:**9868-9876.

43. **Merroun ML, Raff J, Rossberg A, Hennig C, Reich T, Selenska-Pobell S.** 2005. Complexation of uranium by cells and S-layer sheets of *Bacillus sphaericus* JG-A12. Appl. Environ. Microbiol. **71:**5532-5543.

556 44. **Newman DK, Beveridge TJ, Morel F.** 1997. Precipitation of arsenic trisulfide by
557 *Desulfotomaculum auripigmentum*. Appl. Environ. Microbiol. **63:**2022-2028.
558 45. **Beveridge TJ.** 1989. Role of cellular design in bacterial metal accumulation and
559 mineralization. Annu. Rev. Microbiol. **43:**147-171.
560 46. **Evinger M, Agabian N.** 1977. Envelope-associated nucleoid from *Caulobacter*
561 *crescentus* stalked and swarmer cells. J. Bacteriol. **132:**294-301.

562 **TABLES:**

563 **Table 1. Plasmids and bacterial strains used in this study.**

Plasmid/Strain	Description	Reference
Plasmids		
pNPTS138	Non-replicating vector for integration and allelic replacement; *oriT*, *kan* (Km^r), *sacB*	M.R.K. Alley, unpublished
pBXMCS-2	High copy number xylose-inducible expression vector; *kan* (Km^r)	(32)
pRVCHYC-2	Low copy number vanillate-inducible expression vector, contains coding region for a C-terminal mCherry construct; *kan* (Km^r)	(32)
pMCY10	pNPTS138-derived vector for Δ*phoY* allelic replacement	This study
pMCY21	pBXMCS-2-derived vector for expression of *phoY*	This study
pMCY23	pBXMCS-2-derived vector for expression of *phoY-mcherry*	This study
Strains		
C. crescentus		
NA1000	Wild type *C. crescentus*, a synchronizable derivative of CB15	(46)
YJ0010	NA1000 Δ*phoY*	This study
YJ0021	NA1000 Δ*phoY* harboring pMCY21	This study
YJ0023	NA1000 Δ*phoY* harboring pMCY23	This study

564

565

566

567 **Table 2. Primers used in this study.**

Primer	Sequence 5' to 3'
phoY_URfor	GGCTGGCGCCAAGCTTCGGTCACGATATCGGC GACGAG
phoY_URrev	ACGTTGCATATGGCGCAAGAACGGAAGCGT
phoY_DRfor	CGCCATATGCAACGTTGCTAACGGCGGTTAG
phoY_DRrev	CGAAGCTAGCGAATTCATTGAAACGCCCGGCT AGC
BXphoY_for	GGGGAGACGACCATATGTTGCGCGAAGGGCG GCTTC
BXphoY_rev	CGGGCTGCAGGAATTCTTAGCAACGTTGGCCG TAGACCAGC
RVphoY_for	GCGAGGAAACGCATATGTTGCGCGAAGGGCG GCTTC
RVphoY_rev	CGTAACGTTCGAATTCTCGCAACGTTGGCCGT AGACCAGC
BXphoYch_rev	TGGCGGCCGCTCTAGATTACTTGTACAGCTCGT CCATGCCGC

568

569

570 **Table 3. Uranium and phosphate distribution during growth of *C. crescentus* in PYE with**
571 **U.** Uranyl nitrate (200 μM) was added in early-exponential phase, and measurements of soluble
572 and insoluble uranium and phosphate concentrations were taken 30 min after U addition. An
573 abiotic, no cell control was included for comparison. Error bars denote standard deviations from
574 three biological replicates.

	Uranium (μM)		Phosphate (μM)		Mol ratio U/P_i	
	Wt cells	Abiotic	Wt cells	Abiotic	Wt cells	Abiotic
Insoluble	154 ± 2 (81 ± 2%)	108 ± 11 (63 ± 8%)	172 ± 8 (22 ± 1%)	83 ± 11 (13 ± 3%)	0.90 ± 0.04	1.32 ± 0.15
Soluble	36 ± 3 (19 ± 2%)	64 ± 8 (37 ± 6%)	603 ± 6 (78 ± 1%)	543 ± 8 (87 ± 2%)	0.06 ± 0.01	0.12 ± 0.02
Total	190 ± 4 (100%)	172 ± 14 (100%)	775 ± 10 (100%)	626 ± 14 (100%)	0.245 ± 0.003	0.275 ± 0.002

575

576

577 **FIGURES:**

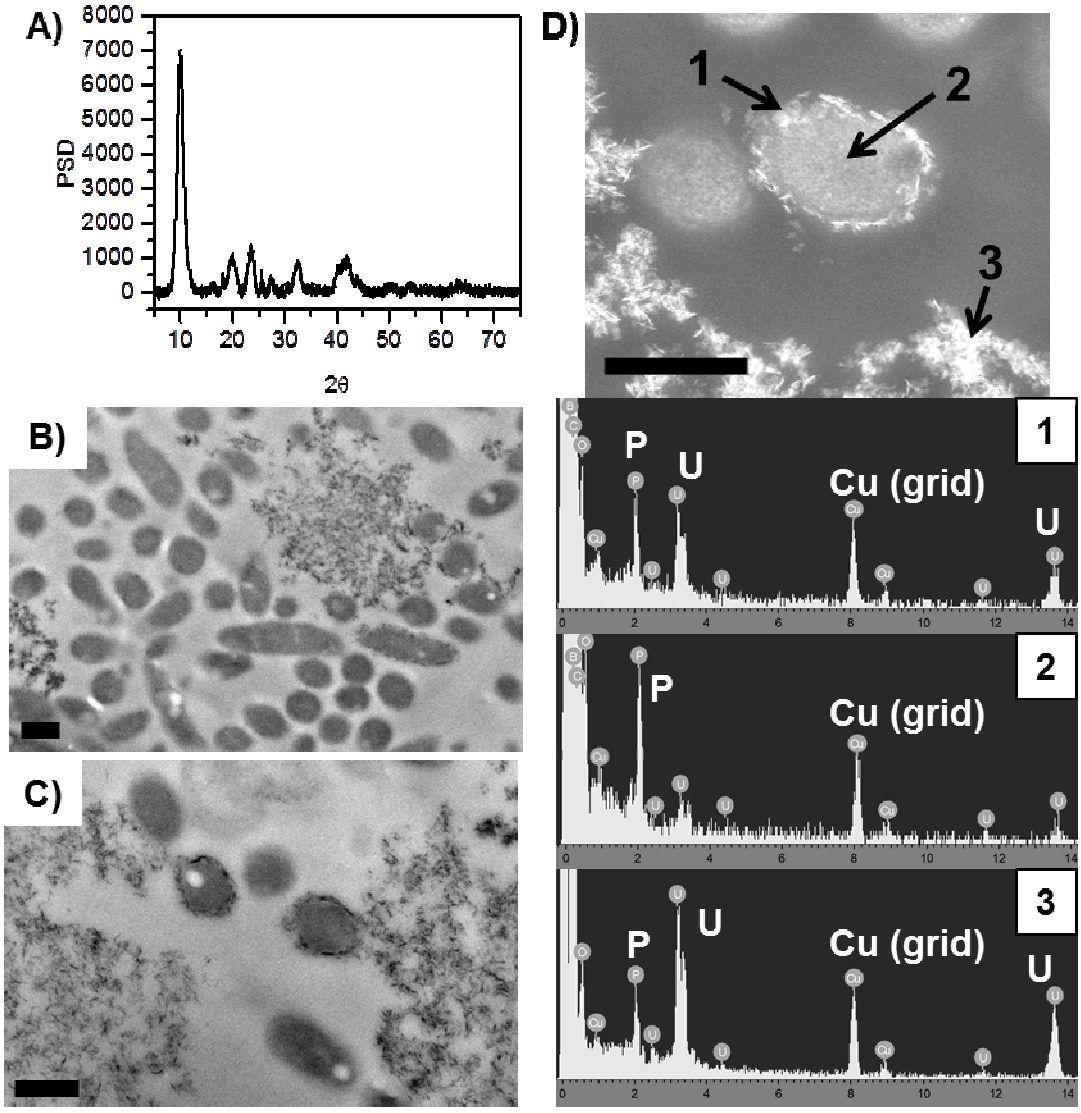

578

579 **Fig 1. XRD and TEM analysis of *C. crescentus* collected during growth in PYE with U.** (A)

580 An XRD spectrum of uranium precipitates. (B and C) Representative TEM images showing U

581 precipitates present on the cell surface and in the bulk medium. Scale bars, 500 nm. C) EDS

582 analysis of areas labeled by arrows in the micrograph above. Scale bar, 500 nm.

583 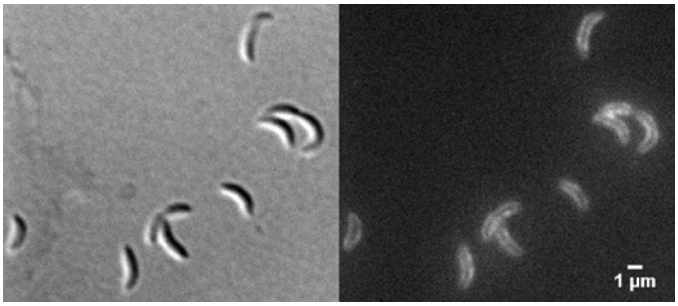

584 **Fig 2. Subcellular localization of PhoY-mCherry.** Δ*phoY* harboring *phoY-mcherry* was
585 grown to early exponential phase in PYE medium supplemented with kanamycin without xylose
586 induction. Bright-field (left) and epifluorescence (right) images are shown. Scale bar, 1 µm.

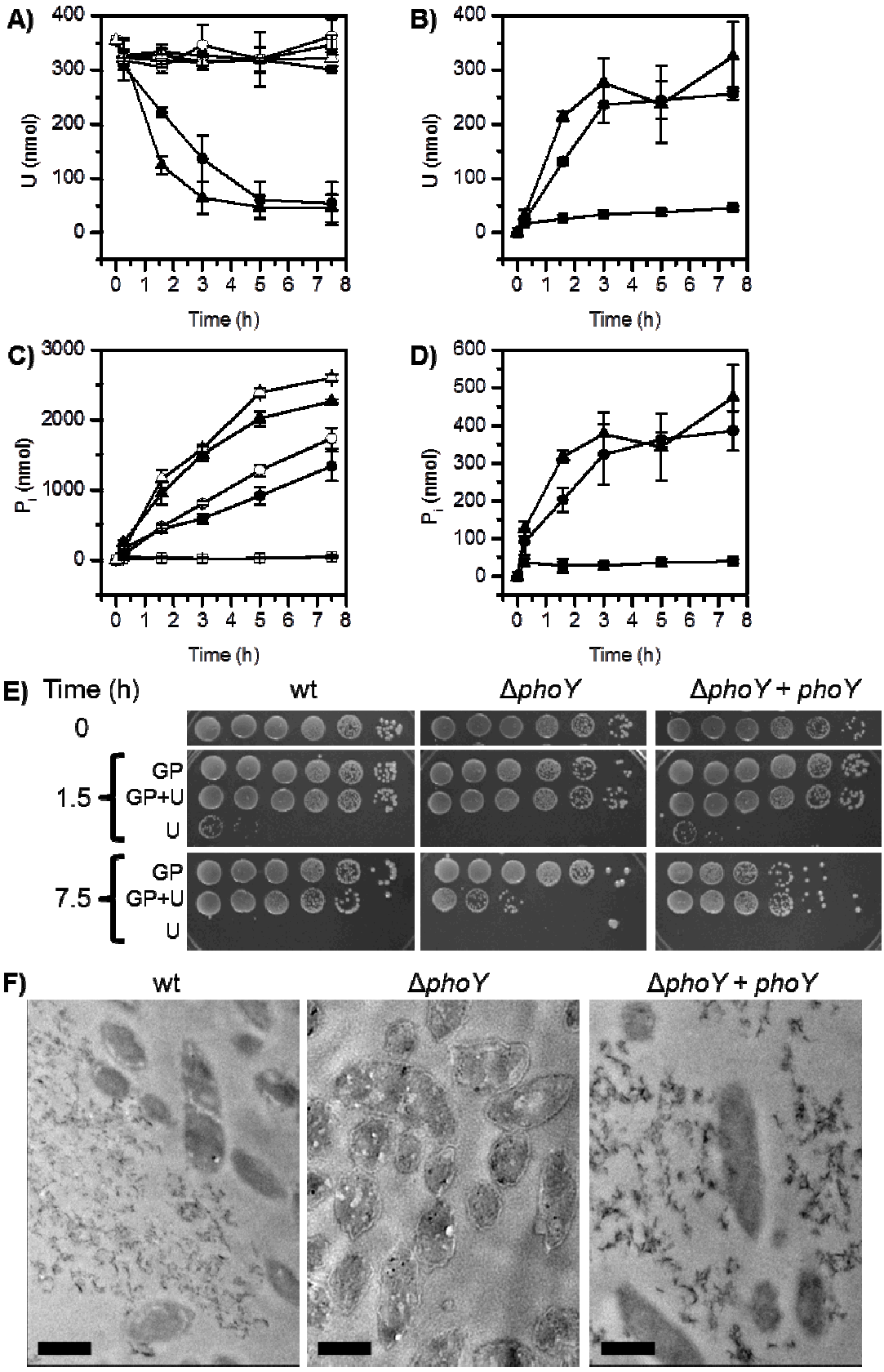
A)
B)
C)
D)
U (nmol)
P_i (nmol)
Time (h)
E) Time (h)
wt
ΔphoY
ΔphoY + phoY
0
1.5
7.5
GP
GP+U
U
F)
wt
ΔphoY
ΔphoY + phoY

587

588 **Fig 3. Comparison of U biomineralization and cell survival among wild type, Δ*phoY*, and**
589 ***phoY* complement strains.** (A) Total and soluble uranium. (B) Insoluble uranium. (C) Total
590 and soluble P_i. (D) Insoluble P_i. Wild type, circles; Δ*phoY*, squares; *phoY* complement strain,
591 triangles. In (A) and (C), empty symbols represent total U or P_i, and solid symbols represent
592 soluble U or P_i. Error bars denote standard deviations from three biological replicates. (E) Cell
593 spotting for survival with samples collected at different time points (denoted on the left) during
594 the biomineralization assay. Controls with glycerol-2-phosphate alone (GP) and uranium alone
595 (U) were included. Serial dilutions of 10^1 to 10^6 (left to right) were spotted on PYE-agar. (F)
596 TEM analysis of samples collected at 5 h during the biomineralization assay. Extracellular U
597 precipitates were observed in wild type and *phoY* complement, but were absent in Δ*phoY*. Scale
598 bars, 500 nm. Wt, Wild type; Δ*phoY*, *phoY* deletion mutant; Δ*phoY*+*phoY*, *phoY* complement
599 strain.

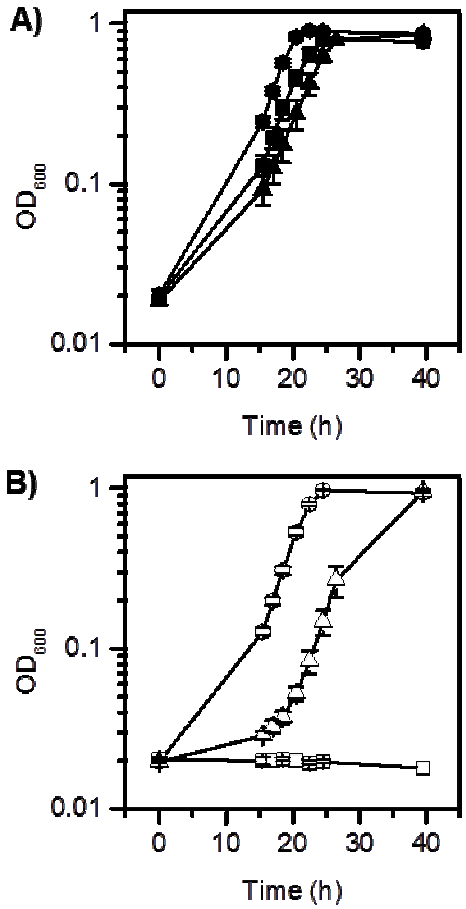

Fig 4. Growth of wild type, Δ*phoY*, and the *phoY* complement strains in M5G-GP medium in the absence (A) or presence (B) of 50 µM uranyl nitrate. Wild type, circles; Δ*phoY*, squares; *phoY* complement strain, triangles. Error bars denote standard deviations from three biological replicates.

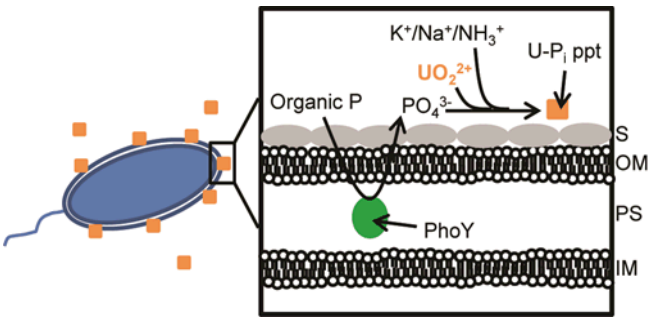

Fig 5. Model for U biomineralization by *C. crescentus*. PhoY, an alkaline phosphatase located in the periplasmic space, catalyzes U biomineralization by cleaving organic phosphate to produce inorganic phosphate, which in turn precipitates with uranyl ion to produce uranium-phosphate precipitates on the cell surface in the form of meta-autunite. S, S-layer; OM, outer membrane; PS, periplasmic space; IM, inner membrane.